NASA Technical Memorandum 113152

Laser Beam Propagation Through Inhomogeneous Media With Shock-Like Profiles: Modeling and Computing

Grigory Adamovsky
Lewis Research Center
Cleveland, Ohio

Nathan Ida
The University of Akron
Akron, Ohio

Prepared for
Optical Technology in Fluid, Thermal, and Combustion Flow III
sponsored by the Society of Photo-Optical and Instrumentation Engineers
San Diego, California, July 27—August 1, 1997

National Aeronautics and
Space Administration

Lewis Research Center

October 1997

Available from

NASA Center for Aerospace Information
800 Elkridge Landing Road
Linthicum Heights, MD 21090-2934
Price Code: A03

National Technical Information Service
5287 Port Royal Road
Springfield, VA 22100
Price Code: A03

Laser beam propagation through inhomogeneous media with shock-like profiles: modeling and computing

Grigory Adamovsky

National Aeronautics and Space Administration
Lewis Research Center
Brookpark Road, Cleveland, Ohio 44135

and

Nathan Ida

The University of Akron
Electrical Engineering Department
Akron, Ohio 44325

ABSTRACT

Wave propagation in inhomogeneous media has been studied for such diverse applications as propagation of radiowaves in atmosphere, light propagation through thin films and in inhomogeneous waveguides, flow visualization, and others. In recent years an increased interest has been developed in wave propagation through shocks in supersonic flows. Results of experiments conducted in the past few years has shown such interesting phenomena as a laser beam splitting and spreading.

The paper describes a model constructed to propagate a laser beam through shock-like inhomogeneous media. Numerical techniques are presented to compute the beam through such media. The results of computation are presented, discussed, and compared with experimental data.

1. INTRODUCTION

Interest in a medium with a rapidly varying refractive index has been increasing recently partially due to the advent of supersonic flight, a growing need for better flow visualization systems and a deeper understanding of light propagation through shocks. In that respect, attempts have been made to explain the refraction phenomenon[1] and formation of refractive fringes[2] and to conduct mathematical and experimental analysis of light diffraction on and transmission through plane shock waves[3,4]. Such phenomena as light diffraction[5] and scattering[6,7] on shocks have been observed and reported. Also, experiments have been performed to determine a normal shock location.[8,9] In view of this development in the experimental field of shocks visualization and analysis a need has arisen for a deeper understanding of the phenomenon of light propagation through a highly inhomogeneous medium. Thus, theoretical and computational models to perform numerical analysis have become important for explaining the recently observed phenomena such as laser beam splitting and broadening.

The purpose of this paper is to present a computational model of a laser beam striking an inhomogeneous body under a grazing incidence. The model includes the inhomogeneous body, the incident laser beam, and a computational scheme to propagate the beam through the inhomogeneity under the grazing incidence.

2. DESCRIPTION OF THE MODEL

To evaluate the phenomenon of wave propagation through inhomogeneous media the following model has been constructed. The inhomogeneous media is assumed to be a penetrable circular cylinder with a cylindrically symmetric profile of the refractive index. The radial distribution of the refractive index profile has a shock-like profile. Such a profile has been described in the literature:[10-13]

$$n(r) = n_{low} + \frac{\Delta n}{1 + exp\left(-4\frac{r-R}{L}\right)}, \tag{1}$$

where

$\Delta n = n_{high} - n_{low}$,

n_{high} and n_{low} are the maximum and minimum values of the refractive index respectively,

R is the radius of the inhomogeneous cylinder,

$r = \sqrt{x^2 + y^2}$ is the radial coordinate,

x and y are Cartesian coordinates of the point of observation,

L is the shock thickness.

Parameters Δn, R, and L describe the shock-like profile of the refractive index. Figure 1 represents an example of a 2-dimensional distribution of the refractive index with $\Delta n = 0.01$, $R = 25\lambda_0$, and $L = \lambda_0$, where λ_0 is the wavelength in vacuum. In this work we assume that $n_{low} = 1$ and $L = 0$. Thus, when $L = 0$, we have a homogeneous cylinder with the index of refraction $n = 1 + \Delta n$ placed in another homogeneous medium with the index of refraction equal to 1.

The cylinder described above is placed in the Cartesian coordinate system with its long axis along the vertical Z axis. It is illuminated by an incident electromagnetic field with the propagation vector normal to the long axis of the cylinder. The electromagnetic field is a sheet of light with a constant intensity in the direction along the axis of the cylinder and the Gaussian intensity profile in the direction normal to it. We will call this sheet of light a laser beam. The electic and magnetic field vectors are chosen to form a transverse magnetic (TM) wave. Assuming that the direction of propagation is the Y direction, the intensity of the two dimensional incident field can be written as:[14,15]

$$E(x,y,t) = A\sqrt{\frac{w_0}{w(y)}}e^{j\varphi(y)}e^{-jky}e^{-\frac{x^2}{w^2(y)}}e^{-jk\frac{x^2}{2R(y)}}e^{j\omega t}, \tag{2}$$

where

$$w(y) = w_0\sqrt{1+\frac{y^2}{y_r}}, \quad R(y) = y + \frac{y_r^2}{y}, \quad \varphi(y) = \frac{1}{2}tan^{-1}\left(\frac{y}{y_r}\right), \quad y_r = \frac{\pi w_0^2}{\lambda}, \tag{3}$$

w_0 is the Gaussian beam waist, and λ is the wavelength of radiation in the medium with refractive index n. Thus $\lambda = \lambda_0/n$, where λ_0 is the wavelength of radiation in vacuum. Coefficient A is a normalization constant.

The beam and the cylinder are positioned in such a way that the optical axis of the beam strikes the cylinder at the grazing incidence at $r = R$. Selection of the described above configuration permits reduction of a three dimensional problem of wave propagation to a two dimensional one.

Selection of a small diameter incident Gaussian beam striking a relatively large diameter scatterer gives an opportunity to separate a scattered field from the incident one. The idea has been implemented for curvature radii measurements.[16] In that experiment a laser beam impinging at a grazing incidence on a surface produced a diffraction edge

wave. A reduction of the laser beam diameter led to a separation of the edge wave from the incident beam. In the region where the two fields overlapped, diffraction fringes were observed.

To compute propagation of the incident beam through the medium described a hybrid method has been selected. The method consists of two parts, propagation through the inhomogeneity and projection of the emerged field into the far field. The first part of the problem, propagation of an electromagnetic field through an inhomogeneity, is computed using the finite-difference time domain (FD-TD) method. The wavefront that emerges as result of calculations then is propagated to a remotely located screen using the Fresnel diffraction equation.

3. FINITE-DIFFERENCE TIME-DOMAIN METHOD

3.1 Introduction

The FD-TD method of computing the electromagnetic wave propagation is based on a simultaneous solution of a system of the first order partial differential equations derived from Maxwell's time dependent curl equations.[17-19] Furthermore, the electric and magnetic field components are positioned in a specific manner described by the Yee algorithm.[20] The algorithm permits solving for both electric and magnetic fields in time and space rather than solving for the electric field along with a wave equation. Those electric and magnetic components are positioned in space in a specific interleaved way which permits a natural satisfaction of tangential field continuity conditions at the interfaces. Due to the fact that the process of solving partial differential equations in an unbounded domain using discrete techniques involves a truncation of the solution domain, an approximated boundary is introduced at a finite distance from a scatterer. This approximate boundary condition is also called an absorption boundary condition (ABC). The ABCs developed by Mur[21] are specially designed to be used with the FD-TD method. Simultaneous discretization in space and time domains requires temporal stability. The time domain discretization scheme is stable if the ratio of spatial segmentation distance to the time step size satisfies the Courant criterion.[22] A straight forward application of a cubical Yee cell in Cartesian coordinates to curved surfaces leads to stair-case approximation. The resultant stepped edge profile of the approximated surface generates an error. [23] One of the ways to minimize the problem is to make the cells small.

3.2 Numerical implementation

To compute wave propagation using the FD-TD method the scattered field formulation has been chosen. It is based on splitting the total field on the known incident and unknown scattered fields, performing the FD-TD computation of the scattered field, and adding the incident field to it to obtain the total field. For a 2D problem pertaining to the model described in the previous section such formulation in a case of TM wave leads to the following equations:

$$\frac{\partial H_x^{Scattered}}{\partial t} = -\frac{1}{\mu_0} \cdot \frac{\partial E_z^{Scattered}}{\partial y} , \tag{4}$$

$$\frac{\partial H_y^{Scattered}}{\partial t} = \frac{1}{\mu_0} \cdot \frac{\partial E_z^{Scattered}}{\partial x} , \tag{5}$$

$$\frac{\partial E_z^{Scattered}}{\partial t} = \frac{1}{\varepsilon_0 \varepsilon_r} \cdot \left(\frac{\partial H_y^{Scattered}}{\partial x} - \frac{\partial H_x^{Scattered}}{\partial y} \right) + \frac{1-\varepsilon_r}{\varepsilon_r} \cdot \frac{\partial E^{Incident}}{\partial t} . \tag{6}$$

The FD-TD discretization process applied to equations derived from scattered field formulation of TM wave propagation gives the following:

$$E_z^{n+1}(i,j) = E_z^n(i,j) + \frac{C_E}{\varepsilon_r} \cdot \begin{bmatrix} H_y^{n+1/2}(i+1/2,j) - H_y^{n+1/2}(i-1/2,j) \\ -H_x^{n+1/2}(i,j+1/2) + H_x^{n+1/2}(i,j-1/2) \end{bmatrix} + \frac{1-\varepsilon_r}{\varepsilon_r} \cdot \frac{\partial E_z^{Incident}(i,j)}{\partial t} \cdot \Delta t \ , \tag{7}$$

$$H_x^{n+1/2}(i,j+1/2) = H_x^{n-1/2}(i,j+1/2) - C_H\left[E_z^n(i,j+1) - E_z^n(i,j)\right] , \tag{8}$$

$$H_y^{n+1/2}(i+1/2,j) = H_y^{n-1/2}(i+1/2,j) + C_H\left[E_z^n(i+1,j) - E_z^n(i,j)\right] , \tag{9}$$

where coefficients associated with electric and magnetic fields are correspondingly $C_E = \Delta t / (\varepsilon_0 \cdot \Delta)$ and $C_H = \Delta t / (\mu_0 \cdot \Delta)$, and $\Delta = \Delta x = \Delta y$. For simplicity, notations for scattered fields in the equations above are omitted. The absorption boundary conditions used are the Mur's conditions of the 2nd order for the edges of the computational domain and of the 1st order for the corners.

3.3 Computational results

The computational domain is selected to be 60 wavelengths wide in X direction and 80 wavelengths long in the direction of beam propagation, or Y direction. To minimize a negative effect of the stair case approximation the size of space steps is chosen to be 0.1 of the wavelength. This resulted in a two dimensional grid with 600 x 800 grid points. 2000 time steps are used to achieve a steady state of the computed field. The time step is selected according to the Courant criterion to be equal to 0.99 of the Courant number Δt_C. The Courant number for a two-dimensional problem is derived from the Courant stability criterion :

$$\Delta t_C = \frac{\Delta}{\sqrt{2} \cdot c_0} = \Delta \cdot \sqrt{\frac{\varepsilon_0 \mu_0}{2}} , \tag{10}$$

where

$\Delta = \Delta x = \Delta y$ is the distance between the grid points,

$c_0 = 1/\sqrt{\varepsilon_0 \mu_0}$ is the speed light in vacuum,

ε_0 and μ_0 are permittivity and permeability of vacuum respectively.

A two dimensional Gaussian beam having the wavelength $\lambda_0 = 1\mu$ and the waist radius $w_0 = 10\lambda_0$ enters the computational domain located at a distance $y_0 = 200\lambda_0$ from the waist. The cylinder and the Gaussian beam are positioned in the computational domain as presented in Figure 2. The propagation of the beam is in the Y direction in a such way that its directional axis passes through the middle of the computational domain. A cylindrical shape body with the refractive index different from the one of the surrounding medium is placed in the passage of the beam the way described in the previous sections.

Figure 3 shows propagation of the Gaussian beam through a medium which contains a cylinder with the radius $R = 30\lambda_0$ and the maximum refractive index difference between the cylinder and the surrounding medium $\Delta n = 0.005$.

Splitting of the incident Gaussian beam and formation of a double peak and fringes are clearly seen on the picture. The phenomena are caused by a combination of effects. The most significant are the interference between the incident Gaussian beam and the diffracted edge wave and scattering by a dielectric cylinder.

Computed effects of the radius of the cylinder and its refractive index on the wave propagation are presented in Figures 4 through 7. The first two of them, Figures 4 and 5, represent three-dimensional views of Gaussian beams propagated through cylinders similar to the one used to obtain data shown in Figure 3 but for $\Delta n = 0.002$ and $\Delta n = 0.008$ respectively. Calculated intensity distributions at the exit from the computational domain for $\Delta n = 0.002$, 0.005, and 0.008 are presented in Figure 6. Figure 7 shows the effect of a change in the radius R of the cylinder with $\Delta n = 0.005$.

Thus, the calculations have shown that the cylinder radius R and refractive index difference Δn have a significant effect on the relative amplitude of the two main peaks in the intensity distribution. It can be seen from the figures that an increase in any of these parameters leads to an increase in amplitudes of both peaks. Moreover, in response to changes in these parameters, the amplitude of the peak to the right changes more rapidly than the one to the left. Another factor that plays an important role in the intensity distribution is the relative position of the beam and the cylinder.

4. FORMATION OF IMAGE IN THE FAR FIELD

One of the methods to propagate optical fields involves the Fresnel diffraction integral. The integral facilitates propagation of an optical disturbance from one plane with coordinates ξ and η to another one with coordinates x and y and located at a distance z from the first. Applying a conventional technique described by Weaver[24] to a two dimensional problem and maintaining the same coordinate notation as in the previous chapters, the following form of the Fresnel diffraction equation can be derived:

$$\psi_2(x) = \frac{Ke^{jky}}{\sqrt{y}} \int_l \psi_1(\xi) \cdot \exp\left[\frac{jk}{2y} \cdot (x-\xi)^2\right] d\xi \tag{11}$$

where K is the inclination factor.

The last expression can be written in terms of the Fourier transform and then solved numerically. Using the established procedure the following is obtained:

$$\Psi_2(u) = e^{jky} \cdot \Psi_1(u) \cdot e^{-j\pi\lambda y u^2} = \Psi_1(u) \cdot H(u), \tag{12}$$

where

$\Psi_1(u)$ and $\Psi_2(u)$ are the Fourier transforms of $\psi_1(x)$ and $\psi_2(x)$ respectively,

$H(u)$ is the free space transfer function of the system, $H(u) = e^{jky} \cdot e^{-j\pi\lambda y u^2}$.

Thus, the process of propagating an optical field from one location to another consists of three steps. These steps are computing the Fourier transform of the field in the original plane, multiplying it by the free space transfer function, and performing the inverse Fourier transformation of the resultant expression in order to find the field at a new location. To perform the direct and inverse Fourier transformations a Fast Fourier Transform algorithm, based on the Danielson-Lanczos Lemma, and computer codes are adopted from available literature on numerical techniques.[25] Results of propagation are presented in the following figures. In the first series of figures the original field is computed using the FD-TD method and then propagated to distances of $20\lambda_0$ and $40\lambda_0$. Figure 8 shows the intensity distribution at a distance of $20\lambda_0$ for cases when the refractive index difference $\Delta n = 0.005$ and $\Delta n = 0.008$. The radius of the cylinder R in both cases remain the same, $R = 30\lambda_0$. When the distance increases the pattern goes through transformations. The sharp changes in the computed intensity distribution become smoother and eventually disappear.

A phenomenon of beam spreading can be observed by comparing the intensity distributions of an undisturbed or reference Gaussian beam with the one that emerges after propagating through the cylinder. The beam spreading manifests in an increase of the spatial width of the curve that forms the intensity distribution. In Figure 9 the beam spreading can be seen

at the right side of the curve next to the reference Gaussian profile. The cylinder used to compute the data has the following parameters: $R = 30\lambda_0$ and $\Delta n = 0.008$. This phenomenon has already been observed experimentally and published.[9] Figures 10 to 11 show intensity distributions at a distance of $80\lambda_0$ from the exit from the computational domain from FD-TD computations with $\Delta n = 0.005$ and $\Delta n = 0.008$ respectively. The beam splitting and broadening are present. Fringes can also be seen. Increase in the refractive index and/or the radius of the cylinder will lead to enhancement of these phenomena.

5. CONCLUSION

A two-dimensional model and hybrid computational technique have been proposed in this paper to propagate a Gaussian beam through inhomogeneities with shock-like profiles into the far field under a grazing incident condition. Computing of the beam propagation through the computational domain is performed by the FD-TD method . The shape of inhomogeneity is selected to be cylindrical. The resultant fields are then propagated into the far field using the Fresnel diffraction equation and Fourier transformation. The computed patterns show effects of the refractive index and the radius of the cylinder. The patterns of intensity distribution of a Gaussian beam in the far field show beam splitting and spreading. These phenomena have been also observed experimentally. An example of the experimentally obtained intensity profile of a Gaussian beam after passing a bow shock is shown in Figure 12. The experimental setup used was similar to the one described in literature.[6,7] To generate bow shock a cylindrical blunt body was inserted in the supersonic flow. A laser beam sent through the shock under the grazing angle of incidence was projected to a remotely located screen. A CCD camera captured the image of the beam on the screen and displayed the beam intensity profile on a computer screen. The beam intensity profile clearly shows beam splitting and formation of fringes. Thus, the model and computational method are supported by experimental data. Moreover, the phenomenon of beam spreading by a shock may be used as the basis for shock detection.

An extension of the method proposed in this paper into the three-dimensional domain will be one of the first future areas of effort. Inhomogeneous bodies then will be spheres with shock-like profiles of the refractive index and large diameters. To build a three dimensional computational model with geometrical dimensions close to those that appear under real conditions some shortcomings of the presented method have to be overcome. One of the shortcomings comes from the limitations of the FD-TD method. Methods based a phase object approximations[26,27] may help to eliminate those limitations. One of the methods, anomalous diffraction approximation,[28,29] is especially attractive when a phase object has it refractive index close to the one of the surrounding medium. However, the method would have to be modified to include potential refractive effects of the spheres.

Other areas that will deserve future attention involve the large angle scattering and polarization phenomena. In order to increase the field of view and evaluate effects associated with large angle scatter, the inclination factor K has to be closely evaluated. The beam propagation into the far field using the Fresnel diffraction equation is based on a scalar field formulation. This means that polarization of the incident beam is not taken into account. Development of a vector field formulation and an associated computational technique represents a certain interest and challenge.

REFERENCES

1. L. Z. Kriksunov and A. E. Pilev, "Refraction of Laser Beams at a Compression Shock," *Sov. J. Opt. Technol.* **51**, pp. 375-377, 1984.
2. J. A. Waltham, P. F. Cunningham, M. M. Michaelis, R. N. Campbell, and M. Notcutt, "The Application of the Refractive Fringe Diagnostic to Shocks in Air," *Optics and Laser Technol.* **19**, pp. 203-208, 1987.
3. H. J. Pfeifer, H. D. Vom Stein, and B. Koch, "Mathematical and Experimental Analysis of Light Diffraction on Plane Shock Waves," *Proc. of the 9th Inter. Congress on High Speed Photography*, pp. 423-426, 1970.
4. S. I. Hariharan and D. K. Johnson, "Transmission of Light Waves Through Normal Shocks," *Appl. Opt.* **34**, pp. 7752-7758, 1995.
5. G. Adamovsky and J. Panda, "Light Diffraction on Shocks," *Display in the Gallery of Fluid Motion at the 47th Annual Meeting of the Division of Fluid Dynamics of the American Physical Society*, November 20-22, 1994, Atlanta, Georgia.
6. J. Panda and G. Adamovsky, "An Experimental Investigation Of Laser Light Scattering by Shock Waves," 33rd AIAA Aerospace Science Meeting and Exhibit (January 9-12, 1995, Reno, Nevada), Paper # AIAA 95-0518.
7. J. Panda and G. Adamovsky, "Laser Light Scattering by Shock Waves," *Phys. Fluids*, **7**, pp. 2271-2279, 1995.

8. S. I. Hariharan, D. K. Johnson, and G. Adamovsky, "A Theory and Experiments for Detecting Shock Locations," in *Laser Applications and Combustion Diagnostics II*, R. J. Locke, ed., Proc. SPIE **2122**, pp. 195-205, 1994.
9. G. Adamovsky and D. K, Johnson, "Optical Techniques for Shock Visualization and Detection," in *Optical Techniques in Fluid, Thermal, and Combustion Flow*, S. S. Cha and J. D. Trolinger, eds., Proc. SPIE **2546**, pp. 348-357, 1995.
10. A. H. Shapiro, *The Dynamics and Thermodynamics of Compressible Fluid Flows*, Ronald Press, New York, 1953.
11. G. R. Cowan and D. F. Hornig, "The Experimental Determination of the Thickness of a Shock Front in a Gas," *J. Chem. Phys.* **18**, pp. 1008-1018, 1950.
12. E. F. Greene, G. R. Cowan, and D. F. Hornig, "The Thickness of Shock Fronts in Argon and Nitrogen and Rotational Heat Capacity Lags," *J. Chem. Phys.* **19**, pp. 427-434, 1951.
13. J. N. Bradley, "Rotational Relaxation and Shock Front Structure," Chapter VII in *Shock Waves in Chemistry and Physics*, (pp. 204-220), Methuen & Co., London, 1962.
14. A. E. Siegman, *Lasers*, University Science Books, Mill Valley, CA, 1986.
15. P. W. Milonni and J. H. Eberly, *Lasers*, John Wiley & Sons, New York, 1988.
16. P. Langlois, R. A. Lessard, and A. Boivin, "Real-Time Curvature Radii Measurements Using Diffraction Edge Waves," *Appl. Opt.* **24**, pp. 1107-1112, 1985.
17. A.Taflove and K. R. Umashankar, "The Finite-Difference Time-Domain Method for Numerical Modeling of Electromagnetic Wave Interaction with Arbitrary Structures," in *Finite Element and Finite Difference Methods in Electromagnetic Scattering*, M. A. Morgan, Ed., (PIER 2, *Progress in Electromagnetic Research*, Elsevier, New York, 1990), pp. 287-373.
18. A. Taflove, *Computational Electrodynamics: the Finite-Difference Time-Domain Method*, Artech House, Boston, 1995.
19. K. S. Kunz and R. J. Luebbers, *The Finite Difference Time Domain Method in Electromagnetics*, CRC Press, Boca Raton, Florida, 1993.
20. K. S. Yee, "Numerical Solution of Initial Boundary Value Problems Involving Maxwell's Equations in Isotropic Media," *IEEE Trans. Antennas Propag.* **AP-14**, pp. 302-307, 1966.
21. G. Mur, "Absorbing Boundary Conditions for the Finite-Difference Approximation of the Time-Domain Electromagnetic Field Equations," *IEEE Trans. Electromag. Compat.* **EMC-23**, pp. 611-624, 1988.
22. M. A. Morgan, "Principles of Finite Methods in Electromagnetic Scattering," in *Finite Element and Finite Difference Methods in Electromagnetic Scattering*, M. A. Morgan, Ed., (PIER 2, *Progress in Electromagnetic Research*, Elsevier, New York, 1990), pp. 1-68.
23. M. Fusco, "FDTD Algorithm in Curvilinear Coordinates," *IEEE Trans. Antennas Propag.* **AP-38**, pp. 76-89, 1990.
24. H. J. Weaver, *Applications of Discrete and Continuous Fourier Analysis*, John Wiley & Sons, 1983.
25. W. H. Press, S. A. Teukolsky, W. T. Vetterling, and B. P. Flannery, *Numerical Recipes in FORTRAN: The Art of Scientific Computing*, 2nd Edition, Cambridge University Press, 1992.
26. Philip S. Brody and Richard P. Leavitt, "Dynamic Holographic Method of Imaging Objects," *Appl. Opt.* **26**, pp. 913-916, 1987.
27. Francis T. S. Yu, *Introduction to Diffraction, Information Processing, and Holography*, MIT Press, Cambridge MA, 1973.
28. H. C. van de Hulst, *Light Scattering by Small Particles*, Dover Publications, New York, 1981, (Originally published by John Wiley & Sons, New York, 1975).
29. G. L. Stephens, "Scattering of Plane Waves by Soft Obstacles: Anomalous Diffraction Theory for Circular Cylinders," *Appl. Opt.* **23**, pp. 954-959, 1984.

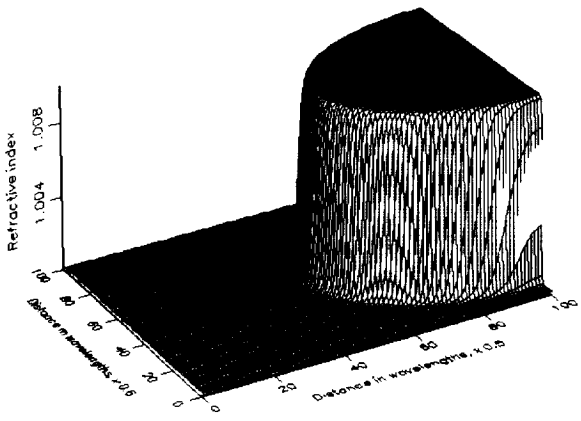

Figure 1: Example of 2D distribution of the refractive index with $\Delta n = 0.01$, $R = 25\lambda_0$, and $L = \lambda_0$.

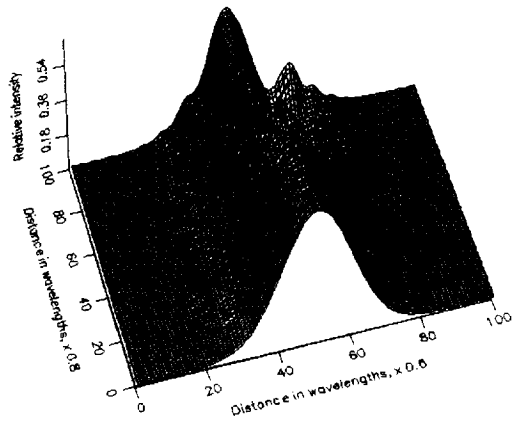

Figure 3: Results of computation of a Gaussian beam propagation through inhomogeneous media with $R = 30\lambda_0$ and $\Delta n = 0.005$; grazing incidence

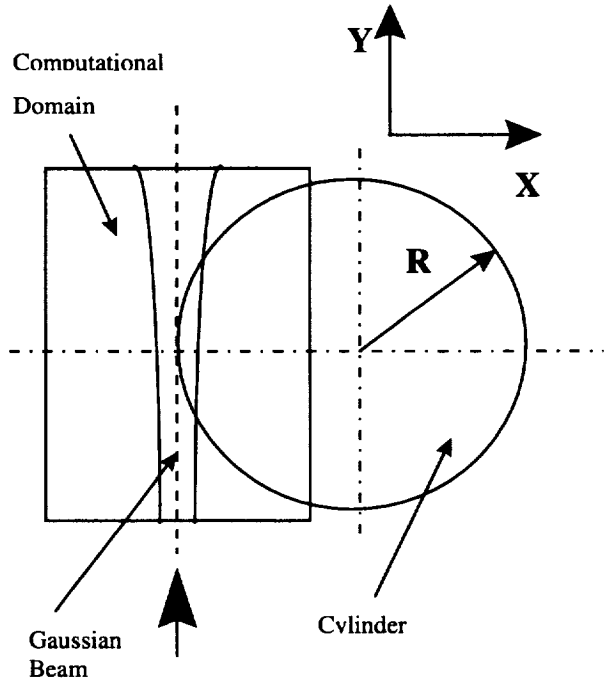

Figure 2: Top view of the computational domain with relative orientation of the incident beam and cylinder; grazing incidence.

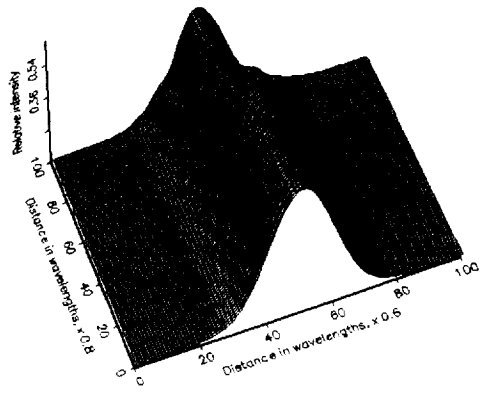

Figure 4: Results of computation of a Gaussian beam propagation through inhomogeneous media with $R = 30\lambda_0$ and $\Delta n = 0.002$; grazing incidence.

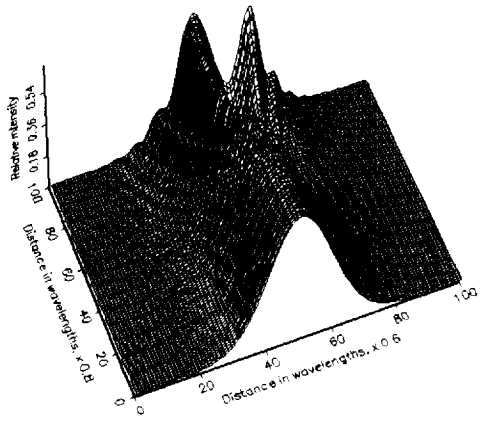

Figure 5: Results of computation of a Gaussian beam propagation through inhomogeneous media with $R = 30\lambda_0$,and $\Delta n = 0.008$; grazing incidence.

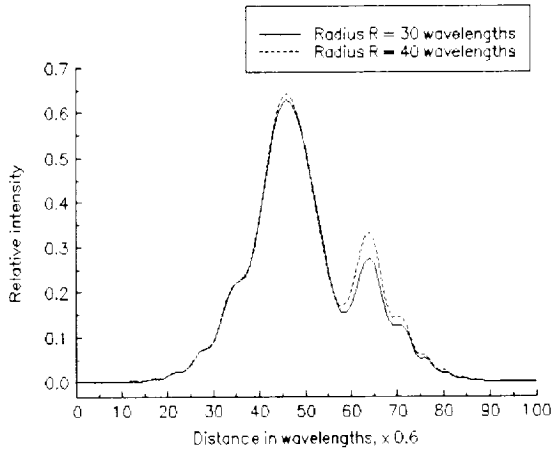

Figure 7: Calculated intensity distributions at the exit from the computational domain for $\Delta n = 0.005$ and different radii R.

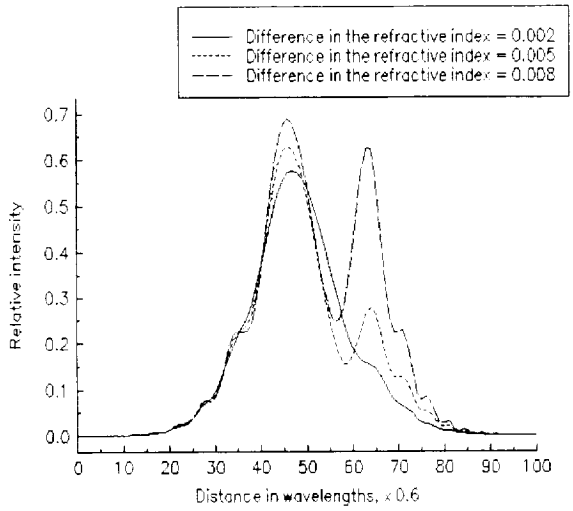

Figure 6: Calculated intensity distribution at the exit from the computational domain for $\Delta n = 0.002$, 0.005, and 0.008; ($R = 30\lambda_0$).

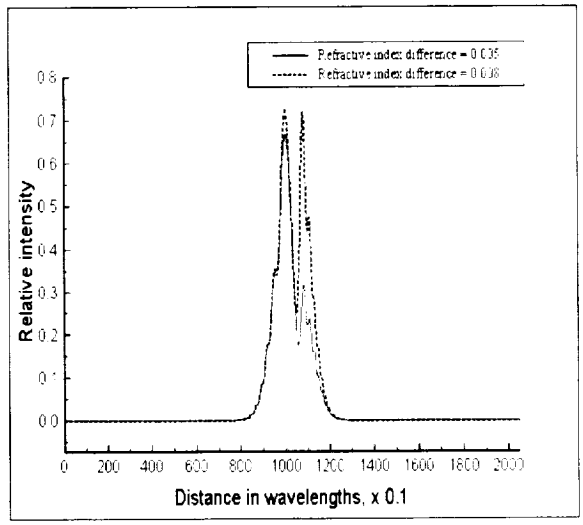

Figure 8: Intensity distribution at $20\lambda_0$ distance for cases of the refractive index differences $\Delta n = 0.005$ and $\Delta n = 0.008$; ($R = 30\lambda_0$).

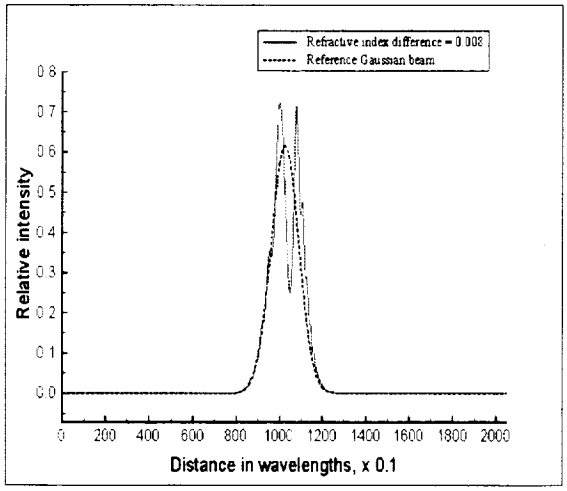

Figure 9: Beam spreading of a Gaussian beam at $20\lambda_0$ distance by a dielectric cylinder ($R = 30\lambda_0$ and Δn = 0.008) under grazing incidence.

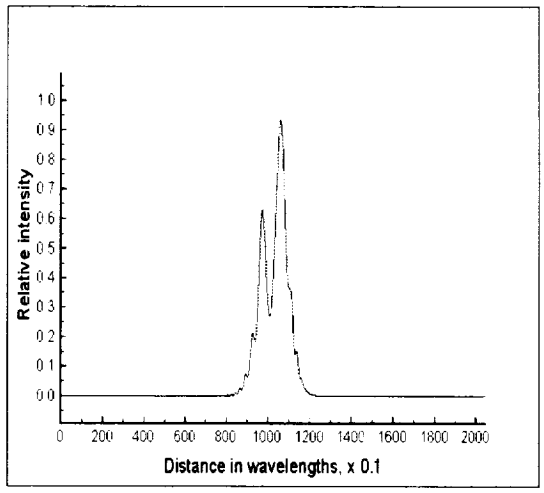

Figure 11: Intensity distribution at $80\lambda_0$ distance obtained using the FD-TD data and Fresnel diffraction equation; ($R = 30\lambda_0$, Δn = 0.008).

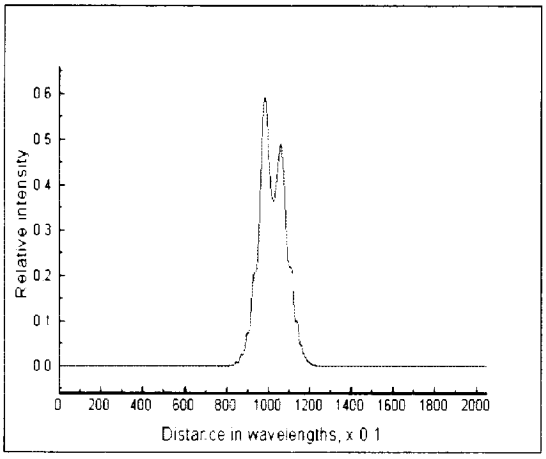

Figure 10: Intensity distribution at $80\lambda_0$ distance obtained using the FD-TD data and Fresnel diffraction equation; ($R = 30\lambda_0$, $\Delta n = 0.005$).

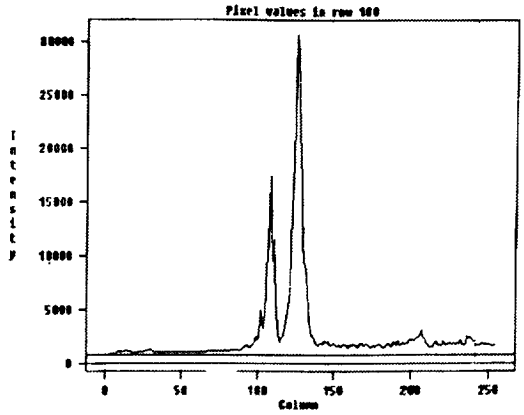

Figure 12: Example of an experimentally obtained intensity profile of a Gaussian beam after passing through a bow shock.

REPORT DOCUMENTATION PAGE

Form Approved
OMB No. 0704-0188

1. AGENCY USE ONLY (*Leave blank*)	2. REPORT DATE	3. REPORT TYPE AND DATES COVERED
	October 1997	Technical Memorandum

4. TITLE AND SUBTITLE

Laser Beam Propagation Through Inhomogeneous Media With Shock-Like Profiles: Modeling and Computing

5. FUNDING NUMBERS

WU-519-20-53

6. AUTHOR(S)

Grigory Adamovsky and Nathan Ida

7. PERFORMING ORGANIZATION NAME(S) AND ADDRESS(ES)

National Aeronautics and Space Administration
Lewis Research Center
Cleveland, Ohio 44135-3191

8. PERFORMING ORGANIZATION REPORT NUMBER

E-10901

9. SPONSORING/MONITORING AGENCY NAME(S) AND ADDRESS(ES)

National Aeronautics and Space Administration
Washington, DC 20546-0001

10. SPONSORING/MONITORING AGENCY REPORT NUMBER

NASA TM-113152

11. SUPPLEMENTARY NOTES

Prepared for Optical Technology in Fluid, Thermal, and Combustion Flow III sponsored by the Society of Photo-Optical and Instrumentation Engineers, San Diego, California, July 27—August 1, 1997. Grigory Adamovsky, NASA Lewis Research Center and Nathan Ida, The University of Akron, Electrical Engineering Department, Akron, Ohio 44325. Responsible person, Grigory Adamovsky, organization code 5520, (216) 433-3736.

12a. DISTRIBUTION/AVAILABILITY STATEMENT

Unclassified - Unlimited
Subject Categories: 74, 64, and 35 Distribution: Nonstandard

This publication is available from the NASA Center for AeroSpace Information, (301) 621-0390.

12b. DISTRIBUTION CODE

13. ABSTRACT ***(Maximum 200 words)***

Wave propagation in inhomogeneous media has been studied for such diverse applications as propagation of radiowaves in atmosphere, light propagation through thin films and in inhomogeneous waveguides, flow visualization, and others. In recent years an increased interest has been developed in wave propagation through shocks in supersonic flows. Results of experiments conducted in the past few years has shown such interesting phenomena as a laser beam splitting and spreading. The paper describes a model constructed to propagate a laser beam through shock-like inhomogeneous media. Numerical techniques are presented to compute the beam through such media. The results of computation are presented, discussed, and compared with experimental data.

14. SUBJECT TERMS

Supersonic flow; Shocks; Flow visualization; FD-TD; Computer modeling; Wave propagation

15. NUMBER OF PAGES

16

16. PRICE CODE

A03

17. SECURITY CLASSIFICATION OF REPORT	18. SECURITY CLASSIFICATION OF THIS PAGE	19. SECURITY CLASSIFICATION OF ABSTRACT	20. LIMITATION OF ABSTRACT
Unclassified	Unclassified	Unclassified	